

# Hydrogenation of thin Y-Ba-Cu-O films: Electrical transport and structure properties of $\text{YBa}_2\text{Cu}_3\text{O}_7$ and $\text{YBa}_2\text{Cu}_4\text{O}_8$

G. Dortmann, J. Erxmeyer, S. Blässer, J. Steiger, T. Paatsch, and A. Weidinger

*Hahn-Meitner-Institut Berlin GmbH, Bereich Schwerionenphysik, Glienicker Strasse 100, D-14109 Berlin, Germany*

H. Karl and B. Stritzker

*Institut für Physik, Universität Augsburg, Memminger Strasse 6, D-86159 Augsburg, Germany*

(Received 4 August 1993)

*c*-axis-oriented  $\text{YBa}_2\text{Cu}_3\text{O}_7$  (1:2:3) and  $\text{YBa}_2\text{Cu}_4\text{O}_8$  (1:2:4) thin films were charged with hydrogen at 463 K and a  $\text{H}_2$  pressure of 100 mbar. The hydrogen concentrations and depth profiles were measured with the  $^{15}\text{N}$  nuclear reaction method. In contrast to earlier studies on bulk samples where a constant  $T_{c,\text{onset}}$  is reported, we find in our 1:2:3 films that the superconducting transition temperature decreases continuously with increasing hydrogen concentration and that the transitions remain relatively sharp, e.g.,  $T_{c,\text{onset}} = 38$  K and  $\Delta T_c = 6.2$  K for  $[\text{H}]/\text{cell} \approx 0.6$ . The electrical resistivity and Hall-effect measurements in the normal state indicate that the main effect of hydrogen doping is a reduction of the charge carrier concentration, whereas the carrier mobility is not changed significantly. At an average hydrogen concentration of  $[\text{H}]/\text{cell} \approx 2$  in both systems, a new hydride phase is observed, which for 1:2:3 is characterized by a *c*-axis expansion of 16% and for 1:2:4 by a *c*-axis expansion of 1.5%.

## I. INTRODUCTION

Since the early work of Reilly's group,<sup>1-3</sup> the subject of hydrogen in high-temperature (high- $T_c$ ) superconductors has been investigated by several research groups.<sup>4-24</sup> There is general agreement that hydrogen reduces the number of charge carriers in *p*-type high- $T_c$  samples and that the material becomes semiconducting and magnetic at high hydrogen concentrations. However, most other questions (e.g., the behavior of  $T_c$  upon *H* charging, structural changes, formation of a hydride phase, etc.) remained unanswered or controversial.

Most of the earlier work was performed on sintered samples or powders<sup>1-18</sup> and only recently studies on thin epitaxial films became available.<sup>20-24</sup> It seems that some of the problems and inconsistencies in the earlier work on bulk samples are connected with inhomogeneities due to different hydrogen concentrations in different parts of the sample. In this respect, epitaxial thin films or single crystals are better suited for such studies.

We report here on our studies on the effect of hydrogen charging on the properties of thin epitaxial Y-Ba-Cu-O films. The main subjects addressed in this paper are hydrogen-induced structural changes, in particular the formation of a hydride phase, and investigations of the electrical transport properties as a function of the hydrogen concentration in the films. We find that the superconducting transition temperature  $T_c$  does not remain constant as reported in the literature but changes continuously with the hydrogen concentration.

In the present experiment the hydrogen concentration in the films was measured by the nuclear reaction ( $^{15}\text{N}$ ) method. In this way not only the absolute overall concentration but also the depth profile is obtained, and

therefore at least a rough information on the homogeneity is available. We have no information on the lateral distribution of hydrogen in the films but this is presumably no problem, since considering the homogeneities of the films a constant lateral distribution can be assumed.

## II. EXPERIMENTAL DETAILS

Thin films of  $\text{YBa}_2\text{Cu}_3\text{O}_7$  (1:2:3 phase) on  $\text{SrTiO}_3$  (100) substrates were prepared by the laser ablation method.<sup>25</sup> A pulsed excimer laser ( $\lambda = 248$  nm,  $\tau = 40$  ns) with a repetition rate of 2 Hz and an energy density of 2 J/cm<sup>2</sup> was used for the ablation from a composite 1:2:3 target in an oxygen atmosphere of 0.3 mbar. During deposition the substrate was heated to 750°C. The films prepared in this way were *c*-axis oriented and superconducting with transition temperatures between 88 and 89 K and transition widths of 0.8 to 1.1 K. The film thicknesses were between 180 and 300 nm.

The  $\text{YBa}_2\text{Cu}_4\text{O}_8$  films (1:2:4 phase) were prepared by the  $\text{BaF}_2$  method, first described by Mankewich *et al.*<sup>26</sup> We used electron-beam evaporation sources for Cu and Y, and a resistively heated effusor for  $\text{BaF}_2$ . A quadrupole mass spectrometer controlled the evaporation rates of all components simultaneously. The three components were coevaporated onto  $\text{SrTiO}_3$  substrates in an oxygen atmosphere of  $2 \times 10^{-5}$  mbar with an evaporation rate of approximately 0.3 nm/s. The substrate was heated to 200°C. The final film thicknesses were between 300 and 400 nm.

After deposition the 1:2:4 films were heat-treated externally.<sup>27</sup> The annealing procedure started with a 40 K/min ramp to 800°C, a dwell time of 30 min using wet oxygen for the fluorine-oxygen exchange reaction followed by a change to dry oxygen. After a 3.5 K/min ramp and a dwell time of 30 min at 450°C, the oven was

switched off and cooled down to room temperature. The oxygen flux during the cycle was approximately 15 ml/min. The films contained both *a*- and *c*-axis oriented regions and had transition temperatures between 81 and 82.5 K and transition widths between 1.5 and 2.2 K.

The films were charged with hydrogen from the gas phase at a hydrogen pressure of 100 mbar and a temperature of 463 K in a small vacuum chamber. Usually the charging process was interrupted every 2 or 4 h for the 1:2:3 film and every 10 h for the 1:2:4 film in order to measure the susceptibility, the electrical resistivity, the Hall constant and x-ray diffraction diagrams. The concentration  $[H]/\text{cell} \approx 2$  was reached after approximately 50 h for the 1:2:3 films and after 135–200 h for the 1:2:4 films. The hydrogen uptake was monitored *in situ* by four probe resistivity measurements.

The final hydrogen concentrations and depth profiles in the films were determined with the  $^{15}\text{N}$  method.<sup>28</sup> Thereby the  $\gamma$  yield of the nuclear reaction  $^1\text{H}(^{15}\text{N}, \alpha\gamma)^{12}\text{C}$  as a function of the incident ion energy was measured with a  $6'' \times 6''$  NaI(Tl) scintillator. The  $^{15}\text{N}$  method can be used only at the end of the whole measurement cycle, since the ion beam damages the film and changes its superconducting and normal-state properties. The concentrations for intermediate charging steps were derived from the resistivity increase assuming a linear increase in the normal-state resistivity with hydrogen concentration.

The ac susceptibility was measured with a high-sensitivity setup especially designed for thin film samples.<sup>29</sup> In our arrangement the films were positioned directly above two planar pickup coils. An external magnetic ac field of 2 Oe with a frequency of 750 Hz was applied parallel to the film surface, and the pickup signal was detected using a lock-in technique. The  $T_{c,\text{onset}}$  is determined by the intersect of two straight lines adjusted to the curves in the transition region and in the region just above  $T_c$ . Errors in the determination of  $T_{c,\text{onset}}$  were within 1–2 K.

The electrical resistivity  $\rho_{ab}$  of the films was measured in the van der Pauw geometry (four probe technique) using pressure contacts at the four corners of the  $10 \times 10\text{-mm}^2$  films. The sample temperature was changed inside a liquid helium vessel by heating the films from 4 to 300 K with a rate of 0.3 to 0.5 K/min. The temperature was monitored by a diode thermometer. The measurements were carried out with a dc current of 100  $\mu\text{A}$ .

The Hall constant  $R_H$  was measured in a fixed magnetic field of 2 T normal to the *a*-*b* plane at several temperatures between 100 and 300 K. The Hall voltage  $V_H$  was determined using the van der Pauw method and a dc current of 100  $\mu\text{A}$ . We checked that  $R_H$  at 100 K remained linear in  $B$  between +2 and -2 T and linear in current between 50 and 150  $\mu\text{A}$ . The error of  $R_H$  is approximately  $\pm 10\%$ . Combining  $R_H$  with the measured resistivity  $\rho_{ab}$ , the Hall mobility defined as  $R_H/\rho_{ab}$  was deduced.

The x-ray experiments were carried out on an automatic powder diffractometer (Siemens D500) equipped with a primary monochromator for  $\text{CuK}_\alpha$  radiation. The diffractograms were recorded at room temperature in the angular range between  $5^\circ$  and  $60^\circ$  ( $2\theta$ ).

### III. RESULTS AND DISCUSSION

Depth profiles of films with different hydrogen concentrations (corresponding to different charging times) are shown in Fig. 1 [fairly homogeneous distributions in Fig. 1(a) and less homogeneous ones in Fig. 1(b)]. The film with the higher *H*-concentration in Fig. 1(a) (charging time: 50 h) was measured first with increasing ion energy ( $\bullet$ ), i.e., from the film surface to the film/substrate interface, and subsequently with decreasing ion energy ( $\circ$ ), i.e., back to the surface. We find a mean *H*-concentration per unit cell of  $[H]/\text{cell} = 2$ . The profile measured with decreasing ion energy is almost the same as with increasing energy indicating that the  $^{15}\text{N}$  method did not change the hydrogen concentration appreciably. The decline of the profile towards the film surface indicates a small release of hydrogen from the film surface.

The other profile in Fig. 1(a) ( $\Delta$ , average concentration  $[H]/\text{cell} = 0.6$ ) was obtained for a different film which was charged only for 26 h. Besides the surface peak, which is due to adsorbates at the surface, an almost homogeneous profile with only a slight decrease of the *H* concentration with film depth is observed. In both films, the *H* concentration fall off at the film/substrate interface extends over

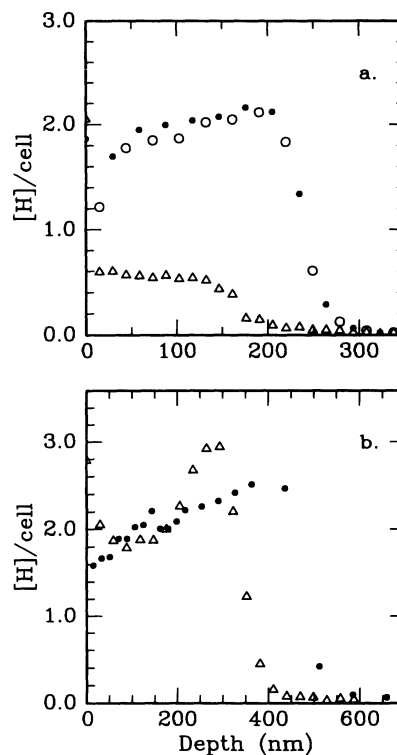


FIG. 1. Hydrogen depth profiles in Y-Ba-Cu-O films. (a) Examples of relative homogeneous *H* depth profiles of 1:2:3 phase films: The film with the average concentration of  $[H]/\text{cell} = 2$  was charged approximately 50 h and measured from the film surface to the film/substrate interface ( $\bullet$ ) and subsequently back to the film surface ( $\circ$ ). The film with the average concentration of  $[H]/\text{cell} = 0.6$  was charged approximately 26 h; the surface peak stems from adsorbates at the surface. (b) Examples of inhomogeneous *H* distributions of a 1:2:3 phase film ( $\bullet$ ) and a 1:2:4 phase film ( $\Delta$ ).

a range of 100 nm. This smear out is probably due to a variation of the film thickness over the ion-beam cross section ( $\varnothing=2$  mm) and not to a variation of the concentration in the film or substrate, respectively.

In some films we find quite inhomogeneous depth profiles as shown in Fig. 1(b) for a 1:2:3 phase film ( $\bullet$ , charging time: 50 h) and a 1:2:4 phase film ( $\Delta$ , charging time: 210 h). It is remarkable that the profiles increase with increasing depth. This behavior excludes the explanation that the thermal equilibrium in the diffusion process into the sample is not reached yet. In such a case a decrease of the H concentration with depth would be expected. The actual profiles found here are probably due to inhomogeneities in the films. For the 1:2:4 phase film the inhomogeneities can probably be explained by the growth process of films prepared by the  $\text{BaF}_2$  method. Beyond 200-nm thickness, these films begin to grow in mixed 1:2:3 and 1:2:4 phases.<sup>27,30,31</sup> The pure 1:2:4 phase is presumably confined to regions close to the substrate with an increasing amount of the 1:2:3 phase closer to the film surface. If we assume that the H solubility is different in the two phases, an inhomogeneous profile can be explained. The hydrogen distribution of the 1:2:3 phase film in Fig. 1(b) is probably also due to film inhomogeneities.

Figure 2 shows the real part  $\chi'$  and the imaginary part  $\chi''$  of the ac susceptibility for a 1:2:3 phase film with different hydrogen concentrations. In the uncharged sample ( $d=180$  nm) the transition to superconductivity is sharp with an onset of the transition temperature of

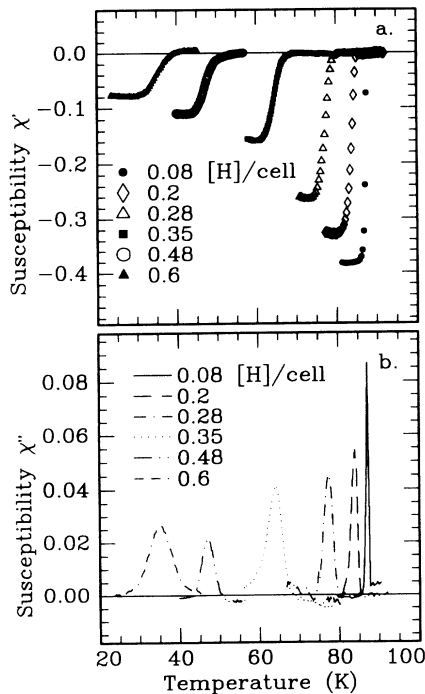


FIG. 2. Real part  $\chi'$  (a) and imaginary part  $\chi''$  (b) of the ac susceptibility (in arbitrary units) as a function of the temperature and hydrogen concentration for a 1:2:3 phase film. The uncharged film already contained an initial hydrogen concentration of  $[\text{H}]/\text{cell} \approx 0.08$ .

$T_{c,\text{onset}}=88$  K and a transition width of  $\Delta T_c=0.8$  K. With increasing hydrogen content,  $T_{c,\text{onset}}$  begins to decrease continuously, whereby the width of the transition remains relatively sharp. The observed reduction in the diamagnetic fraction can be explained by geometric effects due to the finite thickness of the film, since an increase of the London penetration depth with hydrogen charging (due to a reduction in the carrier concentration) leads to a larger volume in which the field can penetrate.

Figure 3 shows the relationship between  $T_{c,\text{onset}}$  and the hydrogen concentration per unit cell. A decrease of  $T_{c,\text{onset}}$  from 88 to 38 K is observed for the hydrogen concentration range up to  $[\text{H}]/\text{cell}=0.6$ , accompanied by an increase of  $\Delta T_c$  from 0.8 to 6.2 K. The  $T_{c,\text{onset}}$  variation is small for  $[\text{H}]/\text{cell} < 0.2$ .

The present finding that  $T_{c,\text{onset}}$  decreases continuously with increasing hydrogen concentration is in marked contrast to earlier reports,<sup>1,4-8</sup> where no change of the onset temperature with hydrogen charging was reported. In these earlier studies the main effect of the hydrogen uptake was an increase of the transition width and a reduction in the diamagnetic fraction. In the light of the present experiment these findings must be interpreted as a result of inhomogeneous samples with a variation of transition temperatures in different regions of the sample. For homogeneously charged samples a fairly unique but reduced  $T_{c,\text{onset}}$  occurs.

Figure 4 shows the temperature dependence of the electrical resistivity  $\rho$  for a hydrogen charged 1:2:3 film. With increasing H content both  $T_c(\rho=0)$  and  $T_{c,\text{onset}}$  decrease in accordance with the susceptibility measurements. Here the transition width increases only from 1 to 3.2 K and  $T_{c,\text{onset}}$  decreases from 90.5 to 65.5 K. The final H concentration was determined as  $[\text{H}]/\text{cell}=0.48$  and a homogeneous depth profile was found. The values of  $T_{c,\text{onset}}$  obtained from the resistivity measurements as a function of the H concentration per unit cell are shown in Fig. 3 together with the susceptibility results. The differences in  $T_{c,\text{onset}}$  obtained by the two methods are presumably a consequence of the different measurement techniques for determining the  $T_{c,\text{onset}}$ . The resistivity is very sensitive to small remaining superconducting re-

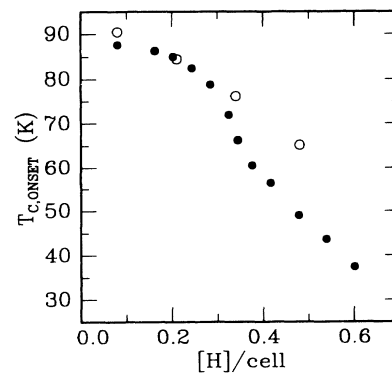


FIG. 3. Relationship between  $T_{c,\text{onset}}$  and the hydrogen concentration per unit cell for a 1:2:3 phase film. Solid circles ( $\bullet$ ) were obtained from ac susceptibility and open circles ( $\circ$ ) from resistivity measurements.

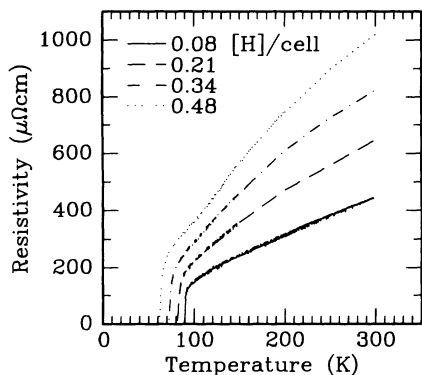


FIG. 4. Temperature dependence of the electrical resistivity  $\rho_{ab}$  for a 1:2:3 phase film for different hydrogen concentrations. As can be seen, the transition to the superconducting state shifts to lower temperature but remains sharp with increasing hydrogen content.

gions, whereas the susceptibility is a bulk property. Thus small inhomogeneities could explain the differences.

The behavior of the normal-state resistivity upon hydrogen charging is also shown in Fig. 4. The resistivity increases upon H charging. It is important to note that mainly the slope of  $\rho$  versus  $T$  increases, whereas the extrapolated residual resistivity at  $T=0$  does not change strongly with increasing hydrogen concentration. This behavior is typical for a resistivity change due to a reduction of the charge carriers. An introduction of scattering centers—for an example see the irradiation studies by Hensel<sup>32</sup>—would lead to a temperature independent increase of the resistivity and no change in the slope  $d\rho/dT$ .

Figure 5 shows the measurement of the Hall coefficient [Fig. 5(a)] and the Hall mobility [Fig. 5(b)]. In Fig. 5(a) the uncharged sample (●) shows the typical strong linear temperature dependence commonly observed for  $\text{YBa}_2\text{Cu}_3\text{O}_7$  samples.<sup>33</sup> A discussion of this behavior is beyond the scope of the present paper. We find that with increasing H content the value of  $R_H^{-1}$  and the slope  $dR_H^{-1}/dT$  decrease. In contrast, the reciprocal value of the mobility  $\mu_H^{-1}$  does not change significantly with increasing H concentration indicating that the mobility of the charge carriers is not affected by the H atoms. This suggests that the H atoms are located at sites where the charge carrier density is low so that no scattering occurs.

On the other hand, a change of the Hall mobility was observed in a study of the Hall parameters of Zn-doped  $\text{YBa}_2\text{Cu}_3\text{O}_7$  single crystals by Chien, Wang, and Ong.<sup>34</sup> Zn is believed to substitute for Cu in the  $\text{CuO}_2$  layers and presumably acts as a scattering center. It is therefore expected that a change in the Hall mobility or equivalently Hall angle occurs. This is indeed observed in the Zn-doped samples. Instead in our case,  $R_H^{-1}$  shows a strong variation with hydrogen doping, whereas the Hall mobility is not influenced much. This suggests that the main effect of H doping on the resistivity is a change in the carrier concentration.

X-ray structure studies upon hydrogen charging have been reported before.<sup>22–24</sup> We here present additional

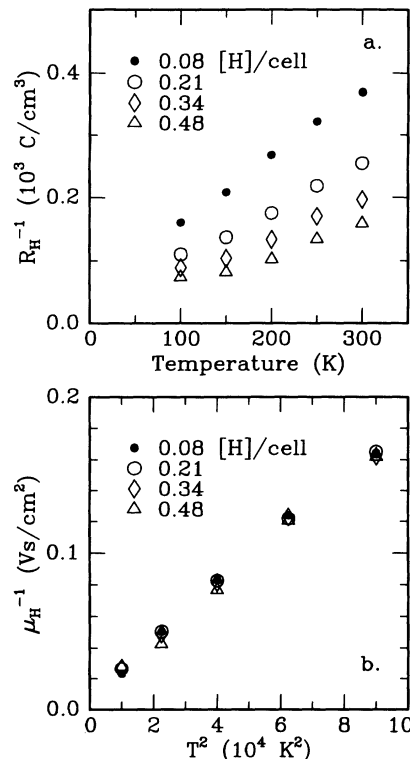


FIG. 5. Temperature dependence of (a) the inverse Hall coefficient  $R_H^{-1}$  and (b) the inverse Hall mobility  $\mu_H^{-1}$  for different hydrogen concentrations.

data on this subject. Furthermore, theoretical calculations for the line intensities have been performed.

Figures 6(a) and 6(b) show the x-ray-diffraction diagrams of the 1:2:3 phase before and after hydrogen charging. The diffractogram in Fig. 6(b) was obtained for an average hydrogen concentration of  $[\text{H}]/\text{cell}=2$  [see upper depth profile in Fig. 1(a)]. The lattice parameter of the hydride phase is  $c=1.365\pm0.003$  nm. At intermediate hydrogen concentrations Paulus *et al.*<sup>24</sup> observed a behavior of the diffraction patterns, which has been explained with a one-dimensional stacking fault sequence in which layers of the unexpanded 1:2:3 phase ( $d_1=1.175$  nm) and layers of the fully expanded, nonsuperconducting phase ( $d_2=1.365$  nm) were randomly distributed. With increasing hydrogen content the number of expanded layers grew at the expense of the nonexpanded layers. The final result after 50 h of hydrogen charging showed a diffractogram such as the one in Fig. 6(b).

Astonishingly the  $c$ -axis lattice parameter of the hydrogenated sample agrees within the experimental errors with the  $c$  axis of the 1:2:4 phase. This leads to the question, whether a new hydride phase is formed or simply the 1:2:4 phase becomes visible upon hydrogen charging, as proposed in the literature.<sup>24</sup> We will argue against the hypothesis that the 1:2:4 phase is observed and instead support the assumption that a hydride phase is formed.

First, the formation of the 1:2:4 phase out of the 1:2:3 phase would require a long-range transport of e.g., Cu atoms; this is very unlikely at the relatively low tempera-

ture of 463 K during hydrogen charging. Secondly, one could assume that 1:2:4 layers are randomly embedded in the 1:2:3 matrix; a fraction of 10% in the as-deposited film would not influence the x-ray diffractogram much. If the 1:2:3 layers were amorphized by hydrogen charging one might argue that as a result the 1:2:4 phase becomes visible in the x-ray diffractogram. However, this is not the case. We have calculated the theoretical diffraction pattern using a modified Hendricks-Teller formalism,<sup>35,36</sup> and found, as expected for the randomness of the 1:2:4 layers, that this kind of transformation does not produce sharp lines as observed in our x-ray diffractograms. Finally, a very important argument in favor of the formation of a genuine new phase is that the line intensities of the diffractograms of the hydrided  $\text{YBa}_2\text{Cu}_3\text{O}_7$  and of  $\text{YBa}_2\text{Cu}_4\text{O}_8$  are different [compare, e.g., Fig. 6(b) and Fig. 9(a)]. In the sample charged with hydrogen we always observed an intensity of the (006) reflection, which is smaller than that of the (004) and (005) reflections. Our measurements on the 1:2:4 phase<sup>22</sup> and those reported in the literature<sup>27,37</sup> always reveal a larger intensity of the sixth reflection than those of the two preceding peaks. From this we conclude that the structure of the new phase is different from the one of the 1:2:4 phase. Note that the  $c$  axis of  $c = 1.53$  nm reported in the study of Fruchart *et al.*<sup>18</sup> is not the same as the one found here.

We further analyzed the structure of the hydride phase and performed theoretical calculations for the line inten-

sities with the program LAZY PULVERIX,<sup>38</sup> which was adapted to our special problem. First the program was successfully tested to prescribe the  $\text{YBa}_2\text{Cu}_3\text{O}_7$  phase as shown in Fig. 7(a). For a simulation of the new phase the  $\text{BaO-CuO}_2\text{-Y-CuO}_2\text{-BaO}$  blocks (see Fig. 8) were first kept unchanged and the expansion of the unit cell by 0.19 nm was carried out in the  $\text{CuO}$ -chain region. The calculations showed already a fair agreement with the measured line intensities. A slightly better fit with our experimental data was achieved by shifting the Ba atoms inside the blocks by 0.012 nm in the direction of the  $\text{CuO}_2$  planes. Figure 7(b) shows the final result of our theoretical calculations in good agreement with our experiment [Fig. 6(b)]. Figure 8 shows a simplified picture of this hydride phase; however, an exact structure refinement has still to be done. Since the expansion of almost 0.2 nm is relatively large, we propose that this increase is accompanied by a reorganization of the chain-O atom. The x-ray data are insensitive to the exact arrangement of the O and H atoms in the  $\text{CuO}$  chain area.

Figure 9 shows the x-ray diffraction diagrams of the 1:2:4 phase.<sup>22</sup> Here, at approximate the same hydrogen concentration of  $[\text{H}]/\text{cell} \approx 2$ , the unit cell expands only about 1.5%. This can be seen at the (0016) reflection in Fig. 9(b), which is shifted by  $1^\circ$  to lower angles whereas the  $\text{SrTiO}_3$  and  $\text{BaF}_2$  lines remain unshifted. We determined a  $c$ -axis lattice parameter of the uncharged film of  $c = 1.362 \pm 0.003$  nm and of the charged film of  $c = 1.382 \pm 0.003$  nm. The most significant change is that the (00 $l$ ) reflections with odd  $l$ 's, which were absent in the

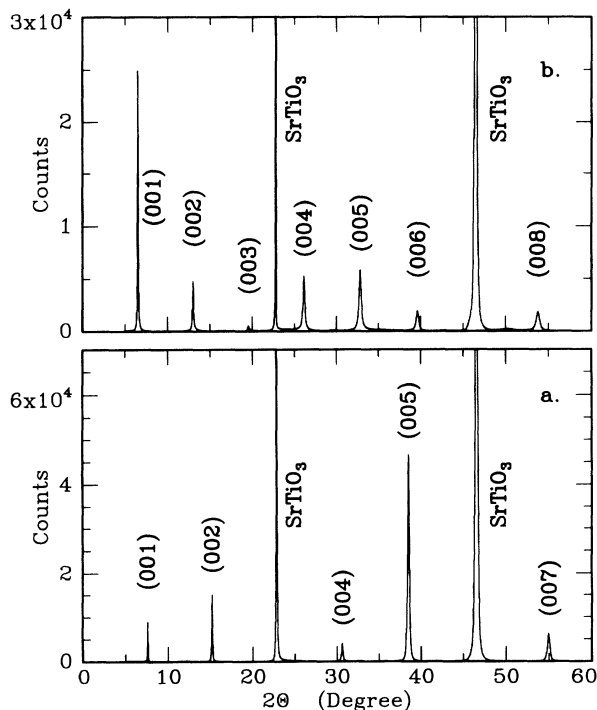


FIG. 6. X-ray diffraction diagrams of a  $c$ -axis-oriented  $\text{YBa}_2\text{Cu}_3\text{O}_7$  film before (a) and after (b) hydrogen charging. The average hydrogen concentration of the charged film is approximately two H atoms per unit cell. The (00 $l$ ) reflections of the lower diffractogram correspond to  $c = 1.175$  nm and those of the upper to  $c = 1.365$  nm. Also indicated in this figure are the reflections of the  $\text{SrTiO}_3$  substrate.

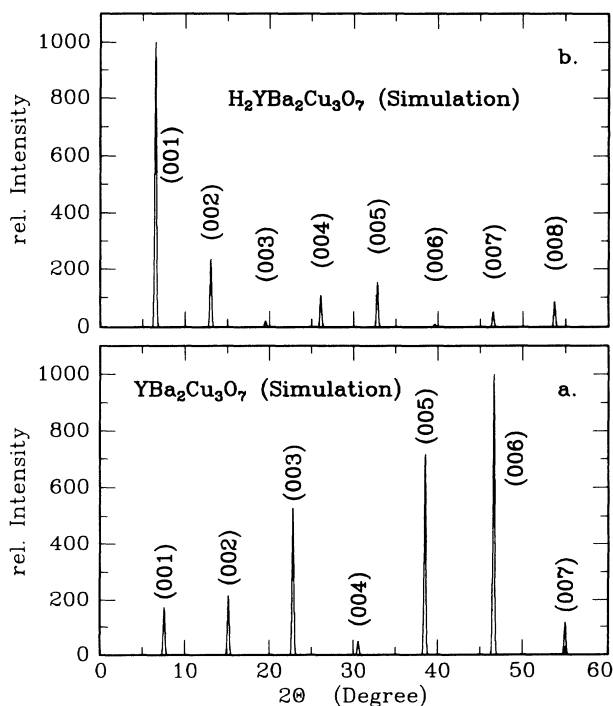


FIG. 7. Calculated intensities of the (00 $l$ ) reflections for the  $\text{YBa}_2\text{Cu}_3\text{O}_7$  phase (a) and the proposed structure (see Fig. 8) for  $\text{H}_2\text{YBa}_2\text{Cu}_3\text{O}_7$  (b). In the calculation for the hydride phase the Ba atoms within the blocks (see Fig. 8) are displaced by 0.012 nm towards the  $\text{CuO}_2$  planes.

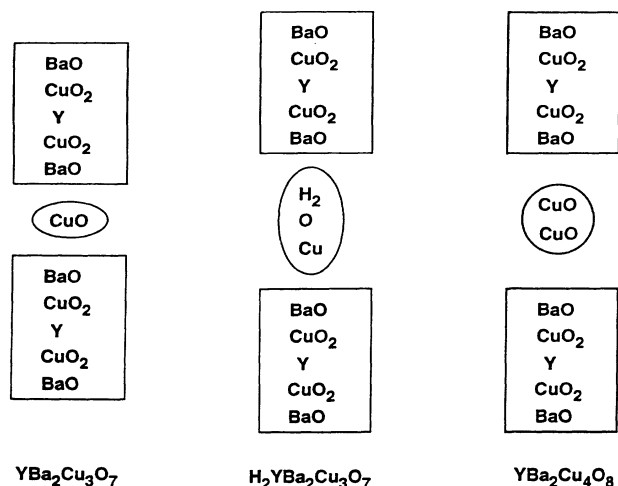


FIG. 8. Proposed structure for the  $\text{H}_2\text{YBa}_2\text{Cu}_3\text{O}_7$  hydride phase. We suggest that the  $\text{BaO-CuO}_2\text{-Y-CuO}_2\text{-BaO}$  blocks remain basically unchanged and that the lattice expansion due to hydrogen uptake occurs in the  $\text{CuO}$  chain area. The present data are insensitive to the detailed arrangement of the  $\text{O}$  and  $\text{H}$  atoms in the chain area.

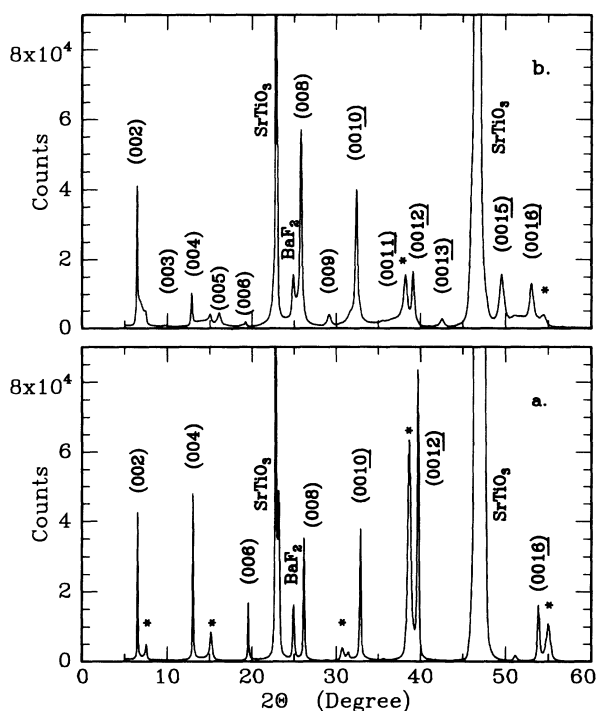


FIG. 9. X-ray diffraction diagrams of the uncharged 1:2:4 film (a) and the film after 135 h of hydrogen charging at 463 K and  $p_{\text{H}_2} = 100$  mbar. The (00l) reflections of the 1:2:4 phase are indicated. The reflections belonging to the 1:2:3 phase are marked by asterisks. Note that in the hydrogen charged film the odd- $l$  reflections are also seen; the (00l) reflections of the hydride phase correspond to an expanded  $c$ -axis lattice parameter of  $c = 2.764 \pm 0.006$  nm.

uncharged film become visible. The absence of these lines in the 1:2:4 phase is due to the fact that two identical layers with only a lateral displacement in the  $b$  axis make up the unit cell. Thus the appearance of the odd- $l$  reflections indicates that this symmetry is destroyed during hydrogen charging. However, the layer structure of the film remains intact; otherwise no sharp reflections would be observed. The relatively small increase of the  $c$  axis in the 1:2:4 phase compared to the 1:2:3 phase can probably be explained with the strong binding of the chain oxygen in 1:2:4. This phase does not tend to rearrange or release oxygen atoms. This fact, on the other hand, supports our hypothesis that in the 1:2:3 phase the chain oxygen  $\text{O}(4)$  is shifted in the  $c$  axis to perform the large expansion of 16%.

#### IV. CONCLUSION

We have studied the effect of hydrogen charging on the electrical transport properties and on the crystal structure of thin Y-Ba-Cu-O films. Most of the earlier work on the hydrogenation of high- $T_c$  superconductors was performed on sintered samples or powders, and often no clear results were obtained. We think that the problems experienced with sintered samples and powders are mainly connected with an inhomogeneous charging, since the hydrogen uptake is strongly influenced by the grain surfaces and the hydrogen concentration may vary for different portions of the sample. For epitaxial films, the starting material for the hydrogenation is much better defined, and therefore a more homogeneous charging can be expected. In addition, in the present case we have controlled the homogeneity at least in one direction by measuring the H-concentration depth profile with the nuclear reaction method.

The main results of the present experiment, which partially deviate from the bulk data, are the following.

(1) The measured changes of the electrical transport properties are consistent with the assumption that hydrogen compensates charge carriers in Y-Ba-Cu-O and thereby reduces the concentration of the carriers. This result is already known from earlier studies on hydrogenated Y-Ba-Cu-O bulk samples by other groups. In addition, we find that the Hall mobility is not strongly influenced by hydrogen charging; thus the built-in protons do not act as scattering centers for the electron transport, probably because the protons are located in the  $\text{CuO}$  chain area, whereas the electrical transport occurs in the  $\text{CuO}_2$  plane region. Contrary to experiments on bulk samples where no change of  $T_{c,\text{onset}}$  with H-charging was observed, we find a clear and continuous decrease of  $T_c$  with H-concentration as expected for a continuous reduction of the charge carrier concentration. We interpret the discrepancy of the bulk data and our finding as an indication of an inhomogeneous H distribution in the bulk samples, which allows for different  $T_c$  values, including the highest ones for almost uncharged portions of the sample.

(2) The second main result concerns the structural changes. A remarkable large expansion of the  $c$ -axis lattice parameter ( $\Delta c/c \approx 16\%$ ) is observed for  $\text{YBa}_2\text{Cu}_3\text{O}_7$

films with an hydrogen concentration of  $[H]=2$  per unit cell. The analysis of the x-ray data for intermediate concentrations<sup>24</sup> implies that either fully expanded or complete nonexpanded layers are formed for a H concentration between 0 and 2. From the present data and from these earlier results we suggest that a stoichiometric hydride phase is formed for  $[H]/\text{cell}=2$ .

(3) For the Y-Ba-Cu-O 1:2:4 phase the results are less clear, since the available films were not single phase. However, we think the main effects concerning the charge carrier compensation and the formation of a hydride phase are the same. A difference is that the lattice expansion in the hydride phase is much smaller ( $\Delta c/c \approx 1.5\%$ ) for the 1:2:4 than for the 1:2:3 phase.

Finally we would like to emphasize that the present

data are not understandable if one assumes, as is sometimes done in the literature, that hydrogenation leads to a decomposition and/or amorphization of the material. In particular, the very clear x-ray data speak strongly against such a hypothesis. The x-ray data are also not consistent with the assumption that hydrogen merely removes oxygen from the sample, since this would not lead to the observed strong *c*-axis expansion. Thus in the present case a hydrogenation of Y-Ba-Cu-O was possible and well-defined structures were formed.

#### ACKNOWLEDGMENTS

We thank B. Mertesacker, J. Bundesmann, and K. Diesner for the help in the experimental work.

- <sup>1</sup>J. J. Reilly, M. Suenaga, J. R. Johnson, P. Thompson, and A. R. Moodenbaugh, *Phys. Rev. B* **36**, 5694 (1987).
- <sup>2</sup>C. Y. Yang, X. Q. Yang, S. M. Heald, J. J. Reilly, T. Skotheim, A. R. Moodenbaugh, and M. Suenaga, *Phys. Rev. B* **36**, 8798 (1987).
- <sup>3</sup>J. R. Johnson, M. Suenaga, P. Thompson, and J. J. Reilly, *Z. Phys. Chem. Neue Folge* **163**, 721 (1989).
- <sup>4</sup>M. Nicolas, J. N. Daou, I. Vedel, P. Vajda, and J. P. Burger, *Solid State Commun.* **66**, 1157 (1988).
- <sup>5</sup>W. Ye, T. Takabatake, T. Ekino, T. Tamegai, and H. Fujii, *Springer Proc. Phys.* **60**, 299 (1992).
- <sup>6</sup>K. Morimoto, W. Ye, S. Orimo, T. Takabatake, H. Fujii, and T. Hihara, *Solid State Commun.* **71**, 291 (1989).
- <sup>7</sup>K. Morimoto, T. Takabatake, W. Ye, S. Orimo, T. Hihara, and H. Fujii, *Physica C* **159**, 849 (1989).
- <sup>8</sup>H. Fujii, H. Kawanaka, W. Ye, S. Orimo, and H. Fukuba, *Jpn. J. Appl. Phys.* **27**, L525 (1988).
- <sup>9</sup>I. Natkaniec, A. V. Belushkin, J. Brankowski, E. A. Goremychkin, J. Mayer, I. L. Sashin, V. K. Fedotov, A. I. Kolesnikov, I. O. Bashkin, V. V. Sinicyn, and E. G. Ponyatovskii, *Physica C* **162-164**, 1369 (1989).
- <sup>10</sup>J. Gross and M. Mehring, *Physica C* **203**, 1 (1992).
- <sup>11</sup>S. D. Goren, C. Korn, V. Volterra, H. Riesemeir, E. Rössler, H. M. Vieth, and K. Lüders, *Phys. Rev. B* **46**, 14 142 (1992).
- <sup>12</sup>S. D. Goren, C. Korn, H. Riesemeir, and K. Lüders, *Phys. Rev. B* **47**, 2821 (1993).
- <sup>13</sup>H. Niki, T. Suzuki, S. Tomiyoshi, H. Hentona, M. Omori, T. Kajitani, T. Kamiyama, and R. Igei, *Solid State Commun.* **69**, 547 (1989).
- <sup>14</sup>H. Niki, H. Hentona, S. Tomiyoshi, M. Omori, T. Kajitani, T. Suzuki, T. Kamiyama, and R. Igei, *Solid State Commun.* **75**, 657 (1990).
- <sup>15</sup>A. M. Balagurov, G. M. Mironova, L. A. Rudnickij, and V. Ju. Galkin, *Physica C* **172**, 331 (1990).
- <sup>16</sup>V. V. Sinitsyn, I. O. Bashkin, E. G. Ponyatovskii, V. M. Prokopenko, R. A. Dilanyan, V. Sh. Shekhtman, M. A. Nevedomskaya, I. N. Kremenskaya, N. S. Sidorov, R. K. Nikolaev, and Zh. D. Sokolovskaya, *Fiz. Tverd. Tela (Leningrad)* **31**, 54 (1989) [*Sov. Phys. Solid State* **31**, 2056 (1989)].
- <sup>17</sup>Ch. Niedermayer, H. Glückler, R. Simon, A. Golnik, M. Rauer, E. Recknagel, A. Weidinger, J. I. Budnick, W. Paulus, and R. Schöllhorn, *Phys. Rev. B* **40**, 11 386 (1989).
- <sup>18</sup>D. Fruchart, J. L. Soubeyroux, D. Tran Qui, C. Pique, C. Rillo, F. Lera, V. Orera, J. Flokstra, and D. H. A. Blank, *J. Less-Common Met.* **157**, 233 (1990).
- <sup>19</sup>H. P. Schölch, M. Weiser, S. Kalbitzer, and G. Saemann-Ischenko, *Jpn. J. Appl. Phys.* **28**, L920 (1989).
- <sup>20</sup>H. Glückler, Ch. Niedermayer, G. Nowitzke, E. Recknagel, J. Erxmeyer, A. Weidinger, and J. I. Budnick, *Europhys. Lett.* **15**, 355 (1991).
- <sup>21</sup>J. Erxmeyer, G. Dortmann, J. Steiger, O. Boebel, and A. Weidinger, *J. Less-Common Met.* **172-174**, 419 (1991).
- <sup>22</sup>G. Dortmann, J. Erxmeyer, and A. Weidinger, *Physica C* **180**, 54 (1991).
- <sup>23</sup>J. Erxmeyer, A. Weidinger, H. Glückler, W. Paulus, R. Schöllhorn, W. Zander, J. Schubert, and B. Stritzker, *Physica C* **185-189**, 1989 (1991).
- <sup>24</sup>W. Paulus, R. Börner, R. Schöllhorn, J. Schubert, W. Zander, J. Erxmeyer, and A. Weidinger, *Adv. Mater.* **4**, 416 (1992).
- <sup>25</sup>B. Stritzker, J. Schubert, U. Poppe, W. Zander, U. Krueger, A. Lubig, and Ch. Buchal, *J. Less-Common Met.* **164-165**, 279 (1990).
- <sup>26</sup>P. M. Mankiewicz, J. H. Scofield, W. J. Skocpol, R. E. Howard, A. H. Dayem, and E. Good, *Appl. Phys. Lett.* **51**, 1753 (1987).
- <sup>27</sup>M. Moske, S. Dina, G. v. Minnigerode, and K. Samwer, *Physica C* **170**, 491 (1990).
- <sup>28</sup>D. A. Leich and T. A. Tombrello, *Nucl. Instrum. Methods* **108**, 67 (1973).
- <sup>29</sup>G. Zibold and D. Korn, *J. Phys. E* **12**, 491 (1979).
- <sup>30</sup>M. P. Siegal, J. M. Phillips, R. B. van Dover, T. H. Tiesel, and J. H. Marshall, *J. Appl. Phys.* **68**, 6353 (1990).
- <sup>31</sup>A. F. Hebard, R. M. Fleming, K. T. Short, A. E. White, C. E. Rice, A. F. J. Levi, and R. H. Eick, *Appl. Phys. Lett.* **55**, 1915 (1989).
- <sup>32</sup>B. Hensel, Ph.D. dissertation, Universität Erlangen, 1990.
- <sup>33</sup>N. P. Ong, in *Physical Properties of the High Temperature Superconductors*, edited by D. M. Ginsberg (World Scientific, Singapore, 1990), Vol. 2, p. 459.
- <sup>34</sup>T. R. Chien, Z. Z. Wang, and N. P. Ong, *Phys. Rev. Lett.* **67**, 2088 (1991).
- <sup>35</sup>S. Hendricks and E. Teller, *J. Chem. Phys.* **10**, 147 (1942).
- <sup>36</sup>D. Hohlwein and W. Metz, *Z. Kristallogr.* **139**, 279 (1974).
- <sup>37</sup>A. Kapitulnik, *Physica C* **153-155**, 520 (1988).
- <sup>38</sup>K. Yvon, W. Jeitschko, and E. Parth, *J. Appl. Crystallogr.* **10**, 73 (1977).